Surface properties and anti-fouling assessment of coatings obtained fromperfluoropolyethersandceramicoxidesnanopowdersdeposited on stainless steel

Valeria Oldani [a,b,*], Rossella del Negro [a], Claudia L. Bianchi [a,b], Raffaella Suriano [c], Stefano Turri [c], Carlo Pirola [a,b], Benedetta Sacchi [a,b]

[a] *Dipartimento di Chimica, Università degli Studi di Milano, via C. Golgi 19, 20133 Milano, Italy*
[b] *Consorzio INSTM, via G. Giusti 9, 50121 Firenze, Italy*
[c] *Dipartimento di Chimica, Materiali e Ingegneria Chimica "Giulio Natta", Politecnico di Milano, Piazza Leonardo da Vinci 32, 20133 Milano, Italy*

Received 6 July 2015
Received in revised form 28 August 2015
Accepted 30 August 2015
Available online 2 September 2015

1. Introduction

Fouling consists in the accumulation of materials on solid surfaces. The formation of thick layers of deposited particles or biofilms usually affects the normal operation of the involved surfaces. Fouling occurs in many industrial devices, like heat exchangers [1], filtrating membranes [2], reactors, combustion engines, but also on marine or water submerged structures, as oil rings or ships hulls [3].

Anti-fouling strategies include the use of protective coatings. In general, anti-fouling or fouling release coatings are made of low energy, hydrophobic/oleophobic materials. Moreover, they should have high chemical and physical stability, in order to prevent the surface energy increase or a loss of mass, above all upon long term water exposure [4,5].

Perfluorinated polymers show very low surface energy and both hydrophobic and oleophobic behavior; furthermore, thanks to the very highly energetic C–F bonds, they are characterized by a remarkable chemical and thermal stability [6–9]. Among all the commercial perfluoropolymers, the inorganic–organic hybrids perfluoropolyethers are able to combine the properties of the fluorinated moiety with the reactiveness of inorganic functional groups; thus, they are able to generate interactions with solid substrates [10,11]. Perfluorinated polymers are widely used for the obtainment of hydrophobic, anti-fouling coatings. In a previous work [12] we investigated the fouling mitigation activity of α,ω-substituted perfluoropolyethers (PFPE) in heat exchangers, observing a minor increase of the fouling resistance due to scaling on the coated heat transfer surfaces. Electroless Ni-Cu-P-PTFE (polytetrafluoroethylene) films on metal surfaces for the heat transfer showed ability to reduce both mineral fouling and biofouling [13,14]. Graft terpolymers coatings, enriched by PFPE, demonstrated a good resistance against bio-foulants adhesion (macroalga *Ulva*) [15]; PFPE patterned coatings on gold substrates were exploited as promising anti-fouling materials in presence of proteins or polymeric nanoparticles as fouling agents [16].

Polymeric coatings suffer however from low mechanical and physical stability; improvements in mechanical strength, heat resistance and scratch resistance can be achieved by combining the

* Corresponding author at: Dipartimento di Chimica, Università degli Studi di Milano, via C. Golgi 19, 20133 Milano, Italy.
E-mail address: valeria.oldani@unimi.it (V. Oldani).

polymeric materials with inorganic compounds [17]. Taurino et al. [18] prepared super-hydrophobic and scratch resistant coatings combining a vinylester resin layer with TiO_2/ZrO_2 inorganic layers and a PFPE layer. Mateus et al. [19] prepared, by thermal spraying, different Al_2O_3/TiO_2-fluoropolymer composite coatings, with the aim to improve scratch resistance and reduce water or gas permeability. Cai et al. [20] observed enhancements in wear resistance of micro- and nano-sized composite coatings of TiO_2 and fluoroalkylsilane; moreover, thanks to their hydrophobic behavior, they were able to minimize $CaCO_3$ deposition on pool boiling surfaces, without interfering with the heat transfer efficiency of the substrates.

In this work, to improve the mechanical resistance of the PFPE coatings, titanium dioxide (TiO_2) and zirconium dioxide (ZrO_2) nanoparticles were applied in multilayer. Usually protective or reinforcing films that consist of ceramic oxides are obtained by a sol–gel procedure [21]; in that case it was explored the possibility to use TiO_2 and ZrO_2 commercial nanoparticles to produce the ceramic oxide layer, deposited below the fluoropolymer film. Before the deposition, TiO_2 and ZrO_2 nanoparticles were surface impregnated with triethoxy(octyl)silane (OTES); the hydrolysis of the triethoxy groups guarantees the formation of strong bonds between the ceramic oxide and the organic molecule that modulate the surface wettability of the ceramic oxide, making it hydrophobic [22]. The coatings preparation method developed is easy to handle and low cost. It consists in the deposition, on a stainless steel surface, of a ceramic oxide layer, by spray-coating, and, consecutively, of a PFPE layer by dip-coating.

Surface morphology and composition of the coatings were investigated by scanning electron microscopy and X-ray photoelectron spectroscopy, respectively. Surface free energy of the coatings was determined by contact angle measurements. The resistance of the multilayer coatings against water erosion and aggressive liquid environments was evaluated and compared to those of simple PFPE coatings, in order to assess the improvements in mechanical or physical resistance thanks to the ceramic oxides layer. Finally it was quantified the ability of both the PFPE and multilayer coatings to reduce $CaSO_4$ deposition on stainless steel surfaces, creating the conditions for particulate fouling in stainless steel tubes.

2. Experimental

2.1. Materials

Stainless steel AISI 316 was employed as solid substrate for the coating deposition. Specifically, plain samples (30 mm × 20 mm) and tubes (internal diameter 8 mm, thickness 1 mm, length 100 mm) were used. Before the coating deposition, all the samples were washed by immersion in sodium hydroxide and acetone. Some stainless steel plain samples were also mechanically polished by using #40 and #80 abrasive paper, and ultrasonically washed in methanol and water for 10 min. All the materials used for coatings preparation are briefly reported in Table 1.

The α,ω-substituted perfluoropolyethers were purchased from Solvey-Specialty Polymers, their commercial names are Fluorolink® S10 and Fluorolink® F10 (briefly indicated in the article as S10 and F10). The polymeric structures of the two polymers are reported elsewhere [9]. In brief, Fluorolink® S10 is a α,ω-triethoxysilane terminated PFPE, the average molecular weight (AMW) is 1800 g/mol. The triethoxysilane functional ending groups are able to interact with the OH– active sites present on the stainless steel surfaces, forming covalent bonds, which promote the adhesion of the S10 coating to the substrate [23]. Fluorolink® F10 is a α,ω-ammonium phosphate terminated PFPE and the AMW is 2700 g/mol. The functional chain-ends groups form polar interactions with the metal surfaces [24,25].

Table 1
List of chemicals used for coatings preparation.

Material name	Specifications
Fluorolink® S10	Commercial α,ω-substituted perfluoropolyether
Fluorolink® F10	Commercial α,ω-substituted perfluoropolyether
TiO_2	Commercial nanopowders (P25 by Degussa)
ZrO_2	Commercial nanopowders (Sigma–Aldrich)
Triethoxy(octyl)silane (OTES)	Silane agent for nanopowders impregnation
Acetic acid	Catalyst for polymers reticulation
2-Propanol	Solvent for coatings formulation
Dichloromethane	Solvent for impregnation step

Titanium dioxide (TiO_2) and zirconium dioxide (ZrO_2) nanopowders were employed to reinforce the polymeric film. TiO_2 nanoparticles were purchased from Degussa (TiO_2-P25); the nanopowders are composed by 25% of the rutile phase and by 75% of the anatase phase. Particles size is about 25 nm and superficial area is 50 m^2/g (manufacturer data). ZrO_2 nanopowders (Sigma–Aldrich) have a particle size <100 nm, while specific surface area is ≥25 m^2/g. All the other reagents were purchased from Sigma–Aldrich (purity ≥98%) and used without further purification.

2.2. Characterization

Contact angle (CA) measurements were performed by a Krüss Easy Drop instrument. Water contact angles were measured using Milli-Q distilled water; the static CA was determined by extrapolating the drop profile using the conic section method for CA up to 100° and the Young–Laplace method for CA inferior than 100°. Surface free energy (SFE) of coated samples was calculated by using the Lewis acid–base approach [26]. Three pairs of SFE-Theta values were obtained for each analysis by using as test liquids diiodomethane, distilled water and formamide. Advancing and receding contact angles were measured by increasing and reducing the volume of a sessile water drop during the drop shape analysis. All the CA values reported in this paper are the average values obtained from at least five different determinations, depositing the liquid drops at different sample locations.

X-ray photoelectron spectroscopy (XPS) was used to investigate the coatings composition. An M-probe apparatus (Surface Science Instruments) was employed; the source was a monochromatic Al Kα radiation. The 1s energy level of contaminant carbon (284.6 eV) was taken as the internal reference for peak shift corrections. Fittings were performed by using Gaussian's peaks, Shirley's baseline and no constraints.

Surface morphologies of samples were investigated by a Scanning Electron Microscope (SEM) LEO ZEISS 1430 at 20 kV and coating thickness and roughness were measured with an optical profilometer (UBM Microfocus Measurement System). The roughness was measured on an area of 0.3 mm × 0.5 mm and the resolution was 500 points/mm. The maximum resolution in the vertical direction was 0.006 μm. All the characterization analyses were performed on coatings deposited on plain samples.

2.3. Coatings preparation and deposition

The commercial PFPEs were applied on stainless steel samples from a water containing solution. In particular 1 wt% of S10 was formulated with 1 wt% of acetic acid (as catalyst for polymer reticulation at high temperature), 20 wt% of 2-propanol and distilled water. F10 formulation was prepared by using 10% wt of polymer, 20 wt% of 2-propanol and distilled water. In such a type of

formulations the polymer is only dispersed in the solvents, to obtain a micro-emulsion, the solution was sonicated for 5 min. PFPE coatings were applied on solid substrates by a dip-coating procedure; samples were immersed inside the PFPE solution for 18 h and subsequently dried in a static stove for 3 h (S10 coating) or 24 h (F10 coating) at a temperature of 383 K.

The surface functionalization of titania and zirconia nanopowders with siloxanes was obtained by mixing 0.5 g of nanopowders in 5 mL of dichloromethane and 0.1 g of OTES. The nanopowders dispersion was stirred for 24 h at room temperature and then heated at 313 K for the solvent evaporation. The functionalized nanopowders of ZrO_2 and TiO_2 (0.05 g) were separately dispersed in 6 mL of 2-propanol by ultrasounds and the solution was sprayed on the stainless steel surfaces; 0.4 mL of each solution were used for coating 100 mm^2 of a plain surface. Coatings were dried in air at room temperature. In the text, the ceramic oxides films obtained by following this procedure are briefly indicated as TiO_2-OTES or ZrO_2-OTES.

Multilayer coatings were obtained by overlapping the TiO_2-OTES or ZrO_2-OTES film deposited on the stainless steel surface with a PFPE film, following the same deposition procedures described above. In the paper, only multilayer coatings obtained with the deposition of S10 have been considered (labeled: TiO_2/S10 and ZrO_2/S10).

2.4. Tests set up

The chemical resistance of the coatings was studied by the immersion of the plain samples in different liquid environments; the coatings deterioration was thus evaluated by comparing the initial water contact angle with the contact angle measured after 1 day, 3 days and 7 days immersion. The effects of the following environments were investigated: water (ions content of the water reported in supporting information, Table S1), acid solutions (hydrochloric acid, HCl, pH 2), alkaline solutions (sodium hydroxide, NaOH, pH 9) and disinfectant solutions (mono/di-chloramines, $CH_2Cl/CHCl_2$, pH 7). The concentrations of the solutions were checked daily, by means of pH measurements and adjusted consequently. Disinfectant solutions were replaced with fresh ones every day in order to keep the concentration of mono-chloramines and di-chloramines stable. The test solutions were kept under moderate agitation during the experimentation; tests were performed at room temperature or in a thermostatic bath at 323 or 343 K. Shear stress tests were performed by flowing water upon the plain coated surfaces. The liquid flowrate was kept at 0.13 m/s and the temperature was 313 K. All the tests were performed for 7 days. The data presented in Section 3 (Figs. 5–7) correspond to the best case results obtained among at least three repeats of the same test. The tests were repeated until the final value of contact angle measured for two samples, treated in the same erosive conditions, were similar (±15°).

The effect of the hydrophobic coatings on foulants adhesion was investigated in particulate fouling conditions. Particulate fouling consists in the continuous deposition of colloidal particles suspended in liquid media. The process depends mainly from particles-liquid and particles-solid interactions, which can lead to a deposition of the particles on solid surface and a re-suspension into the fluid [27]. In general, it is possible to state that particulate fouling occurs on horizontal surfaces because of gravitational settling of relatively large particles [28]. In the fouling tests (Fig. 1), a calcium sulphate ($CaSO_4$) solution was fluxed inside a stainless steel tube sample, kept in horizontal position, whose internal surfaces were coated. The $CaSO_4$ solution (4 g/L concentration) was obtained by mixing an aqueous solution of calcium nitrate tetrahydrate ($Ca(NO_3)_2$) with an aqueous solution of sodium sulphate (Na_2SO_4). The solution was then heated in a 6 L thank at

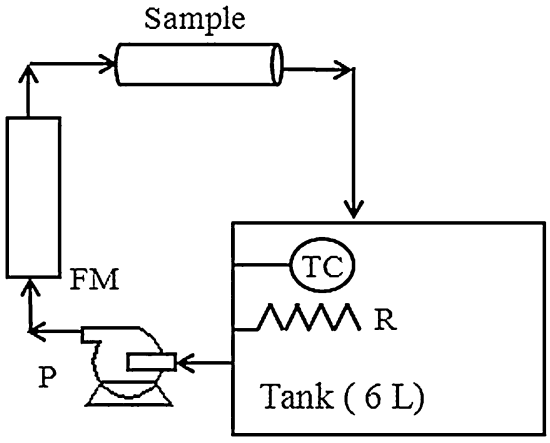

Fig. 1. Schematic of the test-rig used for particulate fouling tests. The $CaSO_4$ solution is heated in the tank and pumped through a metal tube sample whose internal surface was coated. R, heating element; TC, thermocouple; P, pump; FM, float flowmeter.

313 K and the $CaSO_4$ particles precipitated due to supersaturation conditions. The initial concentration of the $CaSO_4$ solution was checked by a titration method; during the test the $CaSO_4$ concentration was not continuously adjusted, since we observed that during the working period selected, the decrease of salt concentration was negligible with respect to the maintenance of the supersaturation conditions. The fluid flowrate was regulated in the range 0.04–0.06 m/s by a float flowmeter (standard accuracy ±5% of full scale flow). Fouling tests were performed for a period varying from 48 to 96 h. The foulant deposition grade was quantified by measuring the sample weight before and after the fouling tests. The weight difference was then normalized in function of the surface area exposed to foulant particles and the time of exposition.

3. Results and discussion

3.1. Coatings morphology, thickness and roughness

X-ray photoelectron spectroscopy analyses were performed on coated stainless steel plain samples. The relative atomic abundance of F and Ti determined on TiO_2/S10 multilayer coatings are 41% and 5% respectively; ZrO_2/S10 multilayer coatings have an atomic composition of F = 38% and Zr = 6%. It is thus possible to suppose the formation of an inhomogeneous layer of the fluorinated polymer upon the ceramic oxide layer. Figs. 2 and 3 report respectively the high resolution spectra of Ti 2p and Zr 3d doublets, in multilayer coatings. Upon the deposition of the fluorinated layer, the typical Ti 2p doublet became more complex, and a two components curve fitting is necessary for correctly interpreting the spectra. Peaks named A and C in Fig. 2 can be referred to Ti(IV) in the oxide, as reported in literature [29].

The second component, expressed by peak *B* and *D*, identifies a titanium oxide species that interacts with a more electronegative species, probably fluorine. Similarly the Zr 3d doublet is very broad and two different Zr components can be identified. Peaks *A* and *C* in Fig. 3 refer to Zr(IV) in the oxide [29], while peaks *B* and *D* correspond to a Zr oxide species interacting with fluorine.

The surface morphology of the coatings was studied by SEM, preparing a S10, F10, TiO_2-OTES, and ZrO_2-OTES layer on different plain samples (Fig. 4b–i); as a reference, the surface morphology of an uncoated stainless steel plain sample was also studied (Fig. 4a). Fig. 4a shows the typical surface morphology of sensitized steel; in particular the grains boundaries were evident because of the

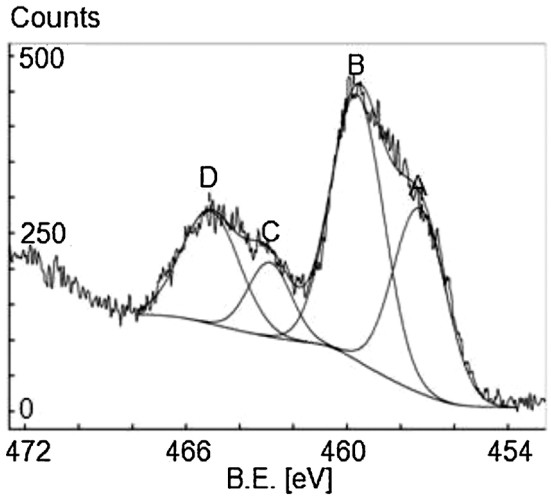

Fig. 2. XPS spectra of the Ti 2p doublet of a TiO_2/S10 multilayer coating. Peak-fit table: *A* = 459.3, *B* = 461.6, *C* = 464.9, *D* = 467.1.

etching procedures, which were performed before the coatings deposition. Both S10 (Fig. 4b, c) and F10 (Fig. 4d, e) layers had an inhomogeneous texture, the coatings were randomly distributed upon the surface and it is possible to recognize the presence of spots not perfectly coated. TiO_2-OTES films, on the other hand, were homogeneous (Fig. 4f); titania nanoparticles formed a compact layer on the solid substrate (Fig. 4g). Similarly ZrO_2-OTES films formed a compact layer upon the stainless steel surface (Fig. 4h), however the nanopowders agglomerated, forming microparticles which generated an inhomogeneous texture (Fig. 4i).

Coatings thickness and roughness were studied by profilometry. The fluorinated layers of S10 and F10 had thickness varying from 3 μm to 5 μm. The ceramic oxides layers had higher thickness, from 20 μm to 25 μm. As expected, multilayer coatings had average thickness of 25–30 μm. The clean stainless steel surfaces had an arithmetic average roughness Ra comprised between 0.174 μm and 0.192 μm; after the deposition of the ceramic oxides layer or the fluorinated layer the surface roughness increased. In particular Ra of the fluorinated layers was 0.438 μm (S10), of a TiO_2-OTES film was 0.786 μm, and of a ZrO_2-OTES film was 0.717 μm. The surface roughness was also measured on a ZrO_2/S10 multi-layer coating, attesting the increase of average roughness of the surface at a value of 0.749 μm.

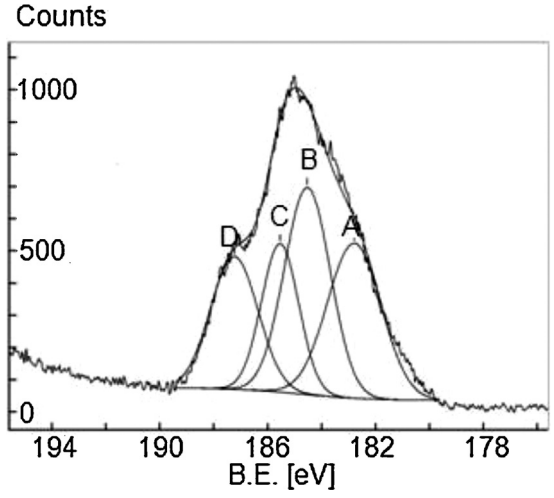

Fig. 3. XPS spectra of the Zr 3d doublet of a ZrO_2/S10 multilayer coating. Peak-fit table: *A* = 182.8, *B* = 184.5, *C* = 185.5, *D* = 187.2.

3.2. Coatings hydrophobicity

Hydrophobicity is the first aspect to be investigated for the assessment of the anti-fouling properties of the coatings. Table 2 lists the surface wetting properties of the various typology of coatings, compared to those of an uncoated stainless steel surface. With respect to an uncoated stainless steel surface, the use of perfluoropolyethers coatings permitted to reduce the surface free energy and to increase the hydrophobicity of the substrate. S10 coatings showed lower surface energy and higher water contact angles than F10 coatings (see Table 2). TiO_2-OTES and ZrO_2-OTES layers, on the other hand, were characterized by a water CA higher than 150°, typical of super-hydrophobic surfaces. The CA hysteresis of these three different types of coatings highlights how the surface roughness affects the wettability of the surfaces. According to the results obtained from profilometer analysis, the lower CA angle hysteresis was detected for the TiO_2-OTES coating, which was characterized by the higher average roughness (Ra = 0.786 μm). By increasing the roughness of these hydrophobic surfaces, in fact, the liquid interacts only with the top of the asperities, since the energy required for following the solid surface profile is higher than the energy associated with the air pockets left inside the texture (this state is described by the Cassie–Baxter equation [30]). The Cassie–Baxter model is suitable to describe the interaction of water with all the coated surfaces here considered, except for the F10 coated surfaces. Here the Wenzel equation could be considered more appropriate for describing the solid/liquid interactions. According to the Wenzel model, the water follows the surface profile and, as a result, the receding contact angle is usually quite inferior to the advancing one, resulting in a large hysteresis [31]. Multilayer coatings reflected the results obtained by the investigation of the single films, i.e., very low surface energy and contact angle hysteresis and very high water contact angles.

3.3. Coatings chemical and physical resistance

The chemical resistance of perfluoropolyethers coatings deposited on stainless steel surfaces was preliminarily assessed and reported in a previous work [12]. In this work we investigated the effect of the surface polishing, performed before the coating deposition, on the PFPE adhesion, comparing this treatment with the reinforcing effect exploited by ceramic oxides nanoparticles.

Alkaline environments degraded in less than 24 h the PFPE films, due to the hydrolysis of the covalent bonds, which formed between the PFPE functional groups or between the functional groups and the solid substrates. Regarding S10 coatings (Fig. 5), chloramines solutions only slightly degraded the hydrophobic films deposited on both polished and unpolished surfaces. The final deterioration corresponds to a 15% decrease of the water CA, which settled after 4 days experimentation. The trend of degradation of the S10 coatings deposited on unpolished surface differed from the one of S10 on polished sample after exposition to HCl solutions (degradation trends are reported in supporting information, Fig. S1). In the former (Fig. 5a), the CA lowly diminishes from the first until the fourth day (5% CA decrease). S10 coating deposited on polished surfaces immediately deteriorates until 9% decrease of the CA (Fig. 5b), which then remained stable for the rest of the experimentation. Different results were obtained after immersion in water. In this case the increasing temperature was responsible of a more pronounced deterioration of the coatings, but, while unpolished coated substrates, after 7 days test, became hydrophilic, polished substrates remained hydrophobic, even if the CA decrease is 35% and the deterioration trend suggests a possible further degradation of the coating for longer immersion time. Also the exposition to a water flow was responsible of a continuous deterioration of the coatings deposited on the unpolished samples

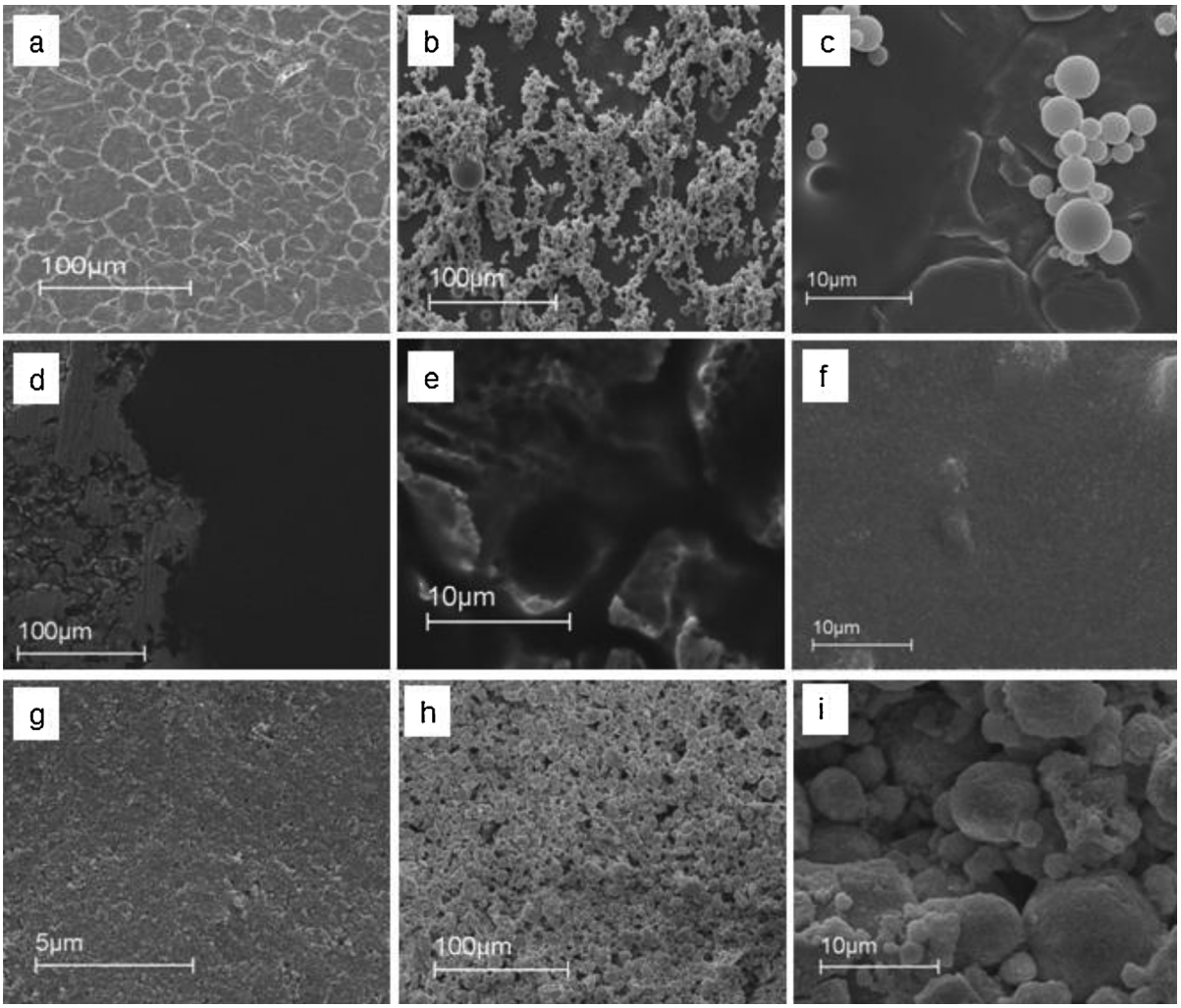

Fig. 4. SEM pictures at 200× (a, b, d, f, h) and 2000× (c, e, g, i) magnification of uncoated stainless steel surface (a); S10 film (b, c); F10 film (d, e); TiO_2-OTES film (f, g); ZrO_2-OTES film (h, i).

(CA < 90°). The CA of the polished substrates coated by S10 mostly decreased within 24 h until the 22%. Comparing Fig. 5a and b, S10 films deposited on polished surfaces showed higher resistance against water erosion at high temperatures and in particular against shear stresses induced by a water flow. Therefore we suppose a better adhesion of the S10 polymer on polished surfaces compared to unpolished ones.

Table 2
Surface wetting properties of stainless steel and coated stainless steel samples.

Coating type	Average static water CA (θ°)	Surface free energy (mN/m)	CA hysteresis
None (unpolished)	76 ± 5.5	45.7 ± 2.0	–
None (polished)	66 ± 4.7	–	–
S10 (polished)	147 ± 2.6	3.3 ± 1.0	6.0
F10 (polished)	123 ± 3.3	11.3 ± 1.2	14.5
TiO_2-OTES	152 ± 0.1	1.8 ± 0.3	0.6
TiO_2/S10	141 ± 2.1	6.4 ± 0.4	2.8
ZrO_2-OTES	156 ± 4.3	7.3 ± 1.0	3.5
ZrO_2/S10	153 ± 3.6	0.85 ± 0.1	1.5

S10, polymeric film made of Fluorolink® S10; F10, polymeric film made of Fluorolink® F10; TiO_2-OTES, single film made of siloxane impregnated TiO_2 nanopowders; ZrO_2-OTES, single film made of siloxane impregnated ZrO_2 nanopowders; TiO_2/S10, multilayer coating made of a siloxane impregnated TiO_2 film and an S10 film; ZrO_2/S10, multilayer coating made of a siloxane impregnated ZrO_2 film and an S10 film.

The starting CA value of the F10 coatings (120–125°) is inferior with respect to the S10 coatings (140–147°); however, the surfaces remained hydrophobic after 7 days of immersion in all the aggressive environments used for the tests, except for NaOH solutions (Fig. 6). The degradation trends were stable and the main deterioration of the coatings occurred within 48 h of immersion for all the conditions adopted (see supporting information, Fig. S2). Moreover, any significant differences were not detected between coatings deposited on polished or not polished samples. Chloramines and hydrochloric acid solutions are the less aggressive solutions against the coatings, as noticed also for S10 films. The CA decrease was 8% for both polished and not polished samples after immersion in chloramines; however the final CA values were inferior than the ones evaluated on S10 coated samples after the same resistance test (≈105° vs ≈140°). The CA measured after immersion in HCl was 15% lower than the starting one in the case of F10 coating deposited on unpolished samples and 7% lower for polished samples. F10 degradation behavior was similar between polished and unpolished samples in the case of immersion in water at high temperature; the coating deterioration occurred within the third day of immersion and consisted in a 20% decrease of the CA value. However the final CA values measured at the end of this test were 98° for the unpolished surface and 95° for the polished one, i.e., the wetting behavior of these surfaces was at the border-line between hydrophobicity and hydrophilicity. The exposition to a

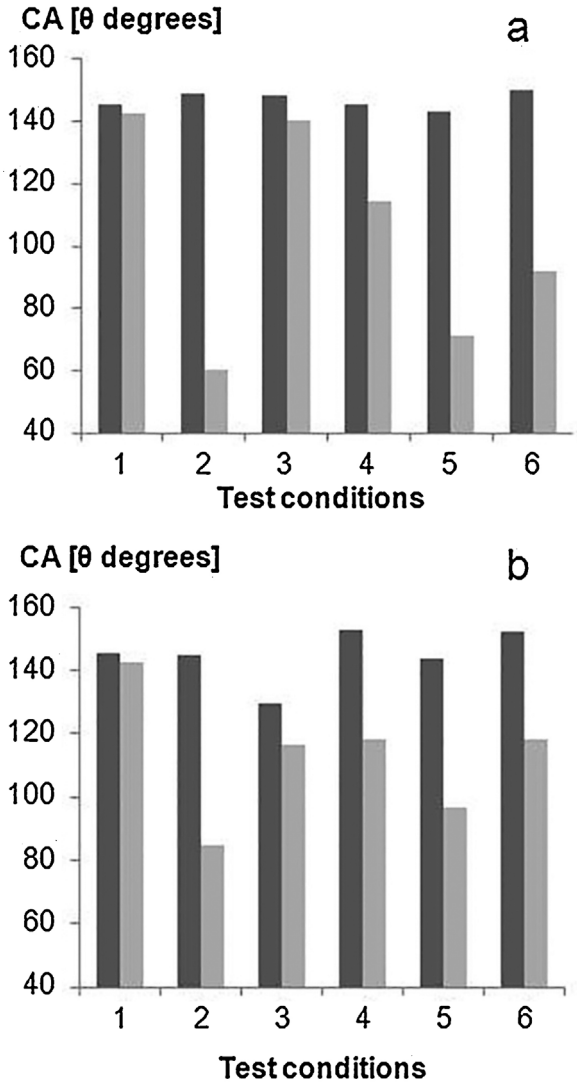

Fig. 5. Coatings resistance tests results for S10 coatings. Comparison between the initial water CA and the water CA measured after 7 days tests of S10 films deposited on unpolished plain samples (a) and polished plain samples (b). ■, initial water CA; ■, final water CA; 1, $NH_2Cl/NHCl_2$ solution, T = 323 K; 2, NaOH solution, T = 323 K; 3, HCl solution, T = 323 K; 4, water, T = 298 K; 5, water, T = 343 K; 6, water flux, T = 313 K, flowrate = 0.13 m/s.

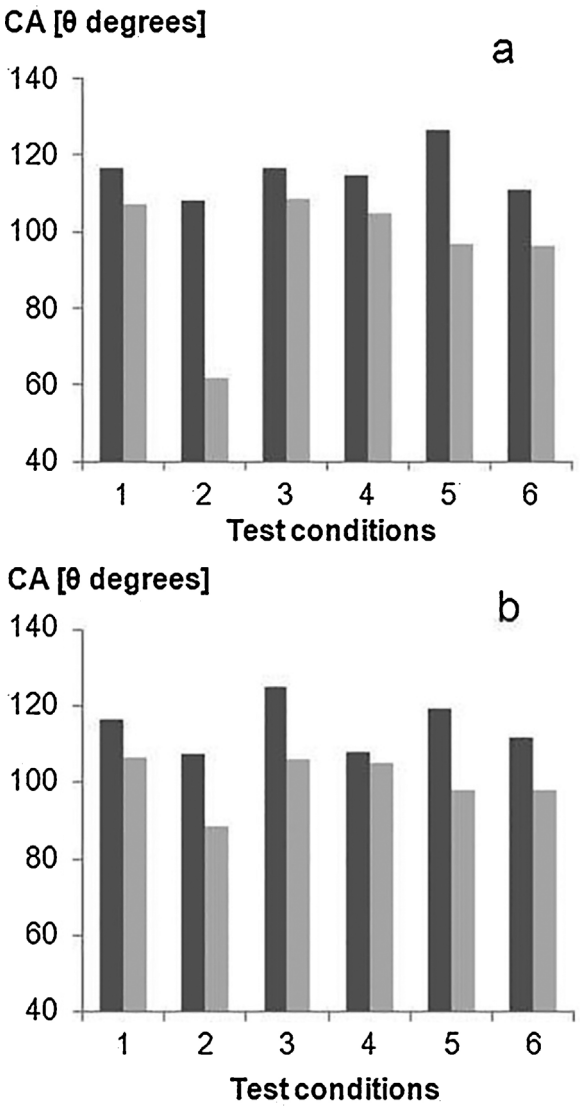

Fig. 6. Coatings resistance tests results for F10 coatings. Comparison between the initial water CA and the water CA measured after 7 days tests of F10 films deposited on unpolished (a) and polished (b) samples. ■, initial water CA; ■, final water CA; 1, $NH_2Cl/NHCl_2$ solution, T = 323 K; 2, NaOH solution, T = 323 K; 3, HCl solution, T = 323 K; 4, water, T = 298 K; 5, water, T = 343 K; 6, water flux, T = 313 K, flowrate = 0.13 m/s.

water flow brought to similar results, the CA decrease is about 15%, but final contact angles are near to 90°, for both polished and unpolished samples treated with F10.

The TiO_2-OTES or ZrO_2-OTES films deposited on stainless steel showed very low resistance against liquid environments, above all at high temperatures; in general after 24 h exposition, the surfaces were completely hydrophilic. Moreover, the exposition to solar light of TiO_2-OTES films brings to an inversion of the super-hydrophobic behavior to a super-hydrophilic one, due in particular to the photocatalytic activity of the TiO_2 anatase phase [30]. The same results were observed on coatings obtained by depositing a ceramic oxide layer upon a S10 film. On the contrary, multilayer coatings obtained by depositing a S10 film on a ceramic oxide film showed improved resistance against aggressive chemicals and shear stresses, compared to single PFPE layers (Fig. 7). TiO_2/S10 coatings are completely degraded by NaOH solutions (Fig. 7a), while ZrO_2/S10 coated surfaces remained hydrophobic; at the end of the test the total CA decrease is 17% (Fig. 7b). Both the multi-layers coatings are resistant against hydrochloric acid and chloramines solutions. TiO_2/S10 showed a stable trend of degradation (supporting information, Fig. S3a); after the first day immersion the CA decrease is 8%, this value was then kept stable until the end of the test. The final CA of ZrO_2/S10 coatings is the 15% inferior to the starting one, but the degradation trend is stable (Fig. S3b). The multilayer coatings deterioration in presence of water is of more complex interpretation. Both TiO_2/S10 and ZrO_2/S10 are low resistant against water at high temperature. TiO_2/S10 coated surfaces became hydrophilic, with a constant degradation of the coating since from the first 24 h of immersion in water at 343 K (Fig. S3c). The CA of ZrO_2/S10 coated surfaces remained stable until the fourth immersion day (Fig. S3d), but after 7 days the surface was hydrophilic. A similar trend was observed for TiO_2/S10 coating after water immersion at room temperature; differently, the ZrO_2/S10 had a final CA decrease of only the 10% (final CA 118°). The deterioration of the multi-layers coatings due to shear stress induced by a water flow is very similar between TiO_2/S10 and ZrO_2/S10. The erosion of the coatings occurred mainly within 24 h exposition to the water flow and the CA

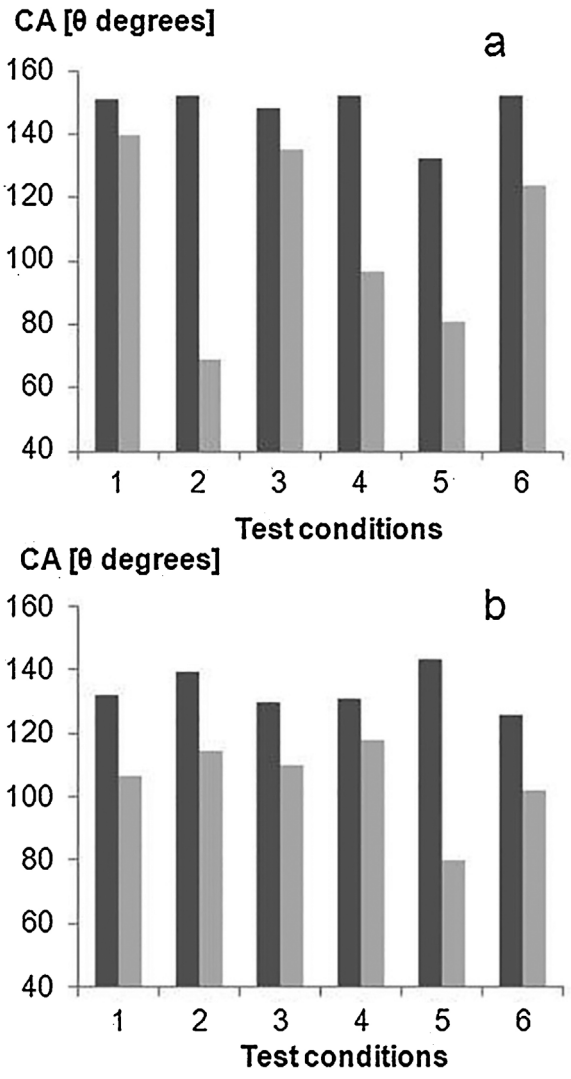

Fig. 7. Coatings resistance tests results for multilayer coatings. Comparison between the initial water CA and the water CA measured after 7 days tests of TiO_2/S10 coatings (a) and ZrO_2/S10 coatings (b). ■, initial water CA; ■, final water CA; 1, $NH_2Cl/NHCl_2$ solution, $T = 323$ K; 2, NaOH solution, $T = 323$ K; 3, HCl solution, $T = 323$ K; 4, water, $T = 298$ K; 5, water, $T = 343$ K; 6, water flux, $T = 313$ K, flowrate = 0.13 m/s.

decrease is ≈19%. No further deterioration was then observed, the CA angle value remained stable after 24 h of immersion. The resistance of multi-layers coatings deposited on polished plain samples was also investigated, however no improvements in coatings resistance were observed.

In brief, the most aggressive liquids for the fluorinated coatings are represented by alkaline solutions and water, in particular at high temperature. The multi-layer coatings showed higher resistance against chemical erosion compared to S10 and F10 fluorinated coatings deposited on unpolished stainless steel surfaces. In respect to fluorinated layers deposited on polished surfaces, multilayer coatings have similar degradation trend. However it has been observed an improvement in resistance against alkaline solution for ZrO_2/S10 coatings, the final contact angle determined was in fact 115°, while S10 or F10 coating suffered a complete deterioration (final contact angle <90°). Moreover multilayer coatings showed higher resistance against shear stresses induced by a water flow, compared to fluorinated layers deposited on both unpolished and polished samples.

Considering the industrial scale, the superficial pre-treatments, such as the stainless steel polishing, are very difficult and expensive. The improvements in mechanical and chemical resistance, observed by the deposition of a ceramic oxide layer before the deposition of the fluoropolymer can be thus considered interesting, in particular for a further development of PFPE-ceramic oxides composite coatings.

Table 3
Determination of $CaSO_4$ deposited on uncoated tubes samples and on coated tubes samples (S10, F10, multilayer coatings).

Coating type	Time (h)	Flowrate (m/s)	Fouling (mg/cm² h)
None	48	0.05	9.2×10^{-5}
None	72	0.05	1.1×10^{-4}
S10	48	0.06	–
S10	72	0.05	1.5×10^{-5}
F10	48	0.05	–
F10	72	0.06	3.0×10^{-6}
TiO_2/S10	48	0.04	2.6×10^{-5}
TiO_2/S10	72	0.06	1.06×10^{-5}
ZrO_2/S10	48	0.04	3.5×10^{-5}
ZrO_2/S10	72	0.05	2.5×10^{-6}

3.4. Particulate fouling test

The deposition of $CaSO_4$ particles on the internal surfaces of stainless steel tubes, during the fouling tests, is expressed as the quantity of foulant particles deposited on the sample surface (mg), in function of the time of exposition (h) and the total internal surface area of the tube sample (cm^2) (Table 3). The $CaSO_4$ concentration adopted in this experimentation guaranteed particles precipitation; the working conditions were not severe, fluid flowrate inside the tubes was in fact kept at low value (≈0.05 m/s) in order to permit a gravitational settling of the large particles onto the horizontal surface. In such a way it was possible to study the foulant deposition in a short period experimentation.

Thanks to the hydrophobic coatings, the $CaSO_4$ adhesion on the stainless steel surface is reduced (Table 3 and Figs. S4 and S5 in supporting information). Foulants adhesion on the coated surfaces was comparable between the single fluorinated layers and the multi-layers coatings, since the surface free energy values were very similar as well. After 48 h test, the weight gain of S10 and F10 coated tubes was zero, an hypotesis is that fouling started after that time. In order to compare the fouling values, we took as a reference the one obtained on the uncoated tube after 72 h of exposition. If this value corresponds to 100% of particles deposition, it results that particulate fouling on S10 coated sample is the 14% and on F10 coated sample is 3% (after 72 h test). Regarding multi-layers coatings, a weight incrementation of the sample was detected after 48 h, anyway the fouling value calculated was inferior than the one determined for the uncoated tube. After 72 h, the fouling was 10% for TiO_2/S10 multilayer coating and 2% for ZrO_2/S10 multilayer coating. Interestingly, the fouling value determined on multilayer coated surfaces after 48 h test is higher than the one determined after 72 h. Since the particulate fouling process consists of deposition phenomena and reentrainment phenomena [26], the fouling decrease observed on multi-layers coated surfaces after the 72 h test can be related to a particles removal. The reentrainment phenomenon depends on the competition between the particles-surface interactions and the particles-fluid interactions. It is possible that the highly hydrophobic behavior of the multilayer coated surfaces influenced the particles-surface interactions, permitting an easier resuspension of the $CaSO_4$ particles deposited on the stainless steel surface.

4. Conclusions

Multilayer coatings for metal surfaces were obtained using a commercial perfluoropolyethers and TiO_2 or ZrO_2 nanoparticles

functionalized by siloxanes. The inorganic layer covered by the PFPE layer worked as a reinforcing film for the organic part. Indeed, by comparing the deterioration of multilayer coatings after exposition to liquids with the one of the simple commercial PFPE coatings, an improvement in mechanical and chemical resistance was observed. We estimated that the CA decrease observed on coatings due to erosion phenomena, is the 15–20% lower for multilayer coatings, in respect to PFPE coatings deposited on the same substrates. Thanks to their hydrophobic behavior, the multilayer coatings find a possible application on fouling protection or mitigation. The deposition of $CaSO_4$ particles during particulate fouling phenomena was studied in coated stainless steel tubes. Both commercial PFPE and multilayer coatings were able to reduce the particles deposition in respect to an uncoated tube; however, it was observed a higher mitigation effect for multilayer coatings: the extent of particulate fouling on stainless steel substrates coated by PFPE is about 10% higher in respect to the one determined on the same substrates coated by multilayer coatings composed by a ZrO_2 film and a Fluorolink® S10 film. This enhanced anti-fouling ability of multilayer coatings is probably due to a higher particle removal phenomenon, induced by the poor particles-liquid/surface interaction.

Appendix A. Supplementary data

Supplementary data associated with this article can be found, in the online version.

References

[1] H. Müller-Steinhagen, M.R. Malayeri, P. Watkinson, Heat exchanger fouling: mitigation and cleaning strategies, Heat Transf. Eng. 32 (2011) 189–196.
[2] L.D. Tijing, Y.C. Woo, J.S. Choi, S. Lee, S.H. Kim, H.K. Shon, Fouling and its control in membrane distillation – a review, J. Membr. Sci. 475 (2015) 215–244.
[3] C.M. Magin, S.P. Cooper, A.B. Brennan, Non-toxic antifouling strategies, Mater. Today 13 (2010) 36–44.
[4] A. Marmur, Super-hydrophobicity fundamentals: implications to biofouling prevention, Biofouling 22 (2006) 107–115.
[5] G.D.Bixler,A.Theiss,B.Bhushan,S.C.Lee,Anti-foulingpropertiesof microstructured surfacesbio-inspiredbyriceleavesandbutterflywings,J. ColloidInterfaceSci.419 (2014)114–133.
[6] M.Vecellio,Opportunitiesanddevelopmentsinfluoropolymericcoatings,Prog. Org. Coat.40(2000)225–242.
[7] C.Tonelli,P.Gavezzotti,E.Strepparola,Linearperfluoropolyetherdifunctional oligomers:chemistry,propertiesandapplications,J.Fluor.Chem.95(1999) 51–70.
[8] W. Navarrini, C.L. Bianchi, L. Magagnin, L. Nobili, G. Carignano, P. Metrangolo, G. Resnati,M.Sansotera,Lowsurfaceenergycoatingscovalentlybondedon diamond-likecarbonfilms,Diam.Relat.Mater.19(2010)336–341.
[9] W.Navarrini,T.Brivio,D.Capobianco,M.V.Diamanti,M.P.Pedeferri,L. Magagnin,G. Resnati,Anti-fingerprintsfluorinatedcoatingforanodized titaniumavoidingcolor alteration,J.Coat.Technol.Res.8(2011)153–160.
[10] M.Messori,M.Toselli,F.Pilati,P.Fabbri,L.Pasquali,M.Montecchi,S. Nannarone,C. Tonelli,Perfluoropolyether-basedorganic-inorganichybrid coatings:preparation andsurfacecharacterization,Surf.Coat.Int.B88(2005) 231–316.
[11] P.Fabbri,M.Messori,F.Pilati,R.Taurino,Hydrophobicandoleophobic coatingsbased onperfluoropolyethers/silicahybridsbythesol–gelmethod, Adv.Polym.Technol.26 (2007)182–190.
[12] V.Oldani,C.L.Bianchi,S.Biella,C.Pirola,G.Cattaneo,Perfluoropolyethers coatings designforfoulingreductiononheattransferstainlesssteelsurfaces, HeatTransf.Eng. (2015),http://dx.doi.org/10.1080/01457632.2015.1044417.
[13] Q. Zhao, Y. Liu, C. Wang, S. Wang, H. Müller-Steinhagen, Effect of surface free energy on the adhesion of bio-fouling and crystalline fouling, Chem. Eng. Sci. 60 (2005) 4858–4865.
[14] Y.H. Cheng, H.Y. Chen, Z.C. Zhu, T.C. Jen, Y.X. Peng, Experimental study on the anti-fouling effects of Ni-P-PTFE deposit surface of heat exchangers, Appl. Therm. Eng. 68 (2014) 20–25.
[15] J.C.Yarbrough,J.P.Rolland,J.M.DeSimone,M.E.Callow,J.A.Finlay,J.A.Callow, Contact angleanalysis,surfacedynamics,andbiofoulingcharacteristicsof cross-linkable, randomperfluoropolyether-basedgraftterpolymers, Macromolecules39(2006) 2521–2528.
[16] S.Kwon,H.Kim,J.Ha,S.Lee,Preventionofproteinandpolymeric nanoparticles adsorptionusingperfluoropolyethers,Ind.Eng.Chem.17(2011) 259–263.
[17] H.Fischer,Polymernanocomposites:fromfundamentalresearchtospecific applications,Mater.Sci.Eng.23(2003)763–772.
[18] R. Taurino, E. Fabbri, D. Pospiech, A. Synytska, M. Messori, Preparation of scratch resistant superhydrophobic hybrid coatings by sol–gel process, Prog. Org. Coat. 77 (2014) 1635–1641.
[19] C.Mateus,S.Costil,R.Bolot,C.Coddet,Ceramic/fluoropolymercomposite coatingsby thermalspraying–amodificationofsurfaceproperties,Surf.Coat. Technol.191 (2005)108–118.
[20] Y.Cai,M.Liu,L.Hui,$CaCO_3$ foulingonmicroscale-nanoscalehydrophobic titania-fluoroalkylsilanefilmsinpoolboiling,AIChEJ.59(2013)2662–2678.
[21] D. Wang, G.P. Bierwagen, Sol–gel coatings on metals for corrosion protection, Prog. Org. Coat. 64 (2009) 327–338.
[22] F. Milanesi, G. Cappelletti, R. Annunziata, C.L. Bianchi, D. Meroni, S. Ardizzone, Siloxane-TiO_2 hybrid nanocomposites. The structure of the hydrophobic layer, J. Phys. Chem. C 114 (2010) 8287–8293.
[23] P.Fabbri,M.Messori,M.Montecchi,F.Pilati,R.Taurino,C.Tonelli,M.Toselli, Surface propertiesoffluorinatedhybridcoatings,J.Appl.Polym.Sci.102 (2006) 1483–1488.
[24] C.L.Bianchi,S.Ardizzone,G.Cappelletti,G.Cerrato,W.Navarrini,M. Sansotera, NanostructuredTiO$_2$ modifiedbyperfluoropolyethers:gasphase photocatalytic activity,J.Mater.Res.25(2010)96–103.
[25] A.Russo,C.Tonelli,E.Barchiesi,Newdevelopmentsinthesynthesisand characterizationofphosphateestersoflinear(per)fluoropolyether monofunctional anddifunctionalmacromonomers,J.Polym.Sci.A:Polym. Chem.43(2005)4790–4801.
[26] C.J. van Oss, R.J. Good, M.K. Chaudhurys, Additive and non-additive surface tension components and the interpretation of contact angles, Langmuir 4 (1988) 884–891.
[27] C. Henry, J.P. Minier, G. Lefèvre, Towards a description of particulate fouling: from single particle deposition to clogging, Adv. Colloid Interface Sci. 185–186 (2012) 34–76.
[28] H. Müller-Steinhagen, H.U. Zettler, in: H. Müller-Steinhagen, H.U. Zettler (Eds.), Heat Exchanger Fouling, Mitigation and Cleaning Technologies, second edition, PP Publico Publications, Israel, 2011, pp. 2–10.
[29] J.F. Moulder, W.F. Stickle, P.E. Sobol, K.D. Bomben, in: J. Chastainc (Ed.), Handbook of X-ray Photoelectron Spectroscopy, Perkin-Elmer Corporation Publication, United States of America, 1992.
[30] A.B.D. Cassie, S. Baxter, Wettability of porous surfaces, Trans. Faraday Soc. 40 (1944) 546–551.
[31] D. Meroni, S. Ardizzone, G. Cappelletti, M. Ceotto, M. Ratti, R. Annunziata, M. Benaglia, L. Raimondi, Interplay between chemistry and texture in hydrophobic TiO_2 hybrids, J. Phys. Chem. 115 (2011) 18649–18658.